CERM

Stereological study of testes following experimentally-induced unilateral cryptorchidism in rats

Javad Sadeghinezhad[1], Fatemeh Yarmahmoudi[1], Mohammad Mehdi Dehghan[2], Saeed Farzad Mohajeri[2], Ehsan Roomiani[1], Hadis Bojarzadeh[1], Mahdi Aghabalazadeh Asl[1], Ava Saeidi[1], Margherita De Silva[3]

Departments of [1]Basic Sciences, [2]Surgery and Radiology, Faculty of Veterinary Medicine, University of Tehran, Tehran, Iran; [3]Department of Veterinary Medical Sciences, University of Bologna, Bologna, Italy

Objective: Cryptorchidism is one of the main causes of infertility and can result in testicular cancer. This study aimed to present quantitative data on the damage caused by cryptorchidism using stereological analysis.

Methods: Thirty newborn rats were randomly divided into control and experimental groups. The experimental group underwent surgery to induce unilateral cryptorchidism in the left testis, whereas the control group underwent a sham surgical procedure 18 days after birth. The testes were removed at designated time points (40, 63, and 90 days after birth) for stereological evaluation and sperm analysis. Total testicular volume, interstitial tissue volume, seminiferous tubule volume and length, and seminiferous epithelium volume and surface area were measured. Other parameters, such as sperm count, sperm morphology, and sperm tail length, were also examined.

Results: Statistically significant differences ($p<0.05$) were observed between the experimental and the control groups at different ages regarding the volumes of various parameters, including the surface area of the germinal layer, the length of the seminiferous tubules, sperm count, and sperm morphology. However, no significant differences were observed in the epithelial volume and the sperm tail length of the groups.

Conclusion: Given the substantial effect of cryptorchidism on different testicular parameters, as well as the irreversible damage it causes in the testes, it is important to take this abnormality seriously to prevent these consequences.

Keywords: Cryptorchidism; Rats; Stereology; Testis

Introduction

The inhibition of testicular descent into the scrotum of one testis (unilateral undescended testis) or both testes (bilateral undescended testes) [1], also known as cryptorchidism, is one of the most common anomalies in the male reproductive system [2] and one of the main causes of infertility [3]. This abnormality affects 3% to 5% of full-term male infants and up to 33% of premature male infants [4]. Moreover, approximately 10% of infertile men undergo surgery for cryptorchidism [5]. The occurrence of cryptorchidism is correlated with hormone levels, assisted reproduction, maternal age, parity, pregnancy-related health, alcohol use, tobacco use (maternal smoking during pregnancy), medication, seasonality, diet, birth presentation, gestational factors, twinning, genetics, and even ethnicity [6]. Intra-abdominal testes are exposed to higher temperatures, and this heat stress causes the sperm mitochondria to produce higher amounts of reactive oxygen species (ROS), which leads to oxidative stress [7]. ROS are known to lead to germ cell depletion and subsequent infertility [8] by inducing apoptosis in spermatogenic cells [9]. Cryptorchidism is also known to cause the production of autoantibodies against the hypothalamic-pituitary axis [10], leading to secondary damage such as testicular cancer. In addition, even though testicular cancer is moderately rare, cryptorchidism is the only confirmed risk factor for testicular germ cell turnover [11].

J Sadeghinezhad et al.   Rat cryptorchid testis stereology

CERM

In most species, including humans, the complete descent of the testes usually occurs prenatally [12]. However, if this process does not occur naturally, this anomaly should be treated with orchiopexy and/or hormonal therapy. Early treatment prevents prolonged damage [13].

Due to the importance of this phenomenon, many studies have been conducted to find effective solutions for cryptorchidism. As of this study, the effects of cryptorchidism on the testis have been evaluated using histology [14,15] and immunohistochemistry [16], yielding valuable insights. However, these methods are limited since they do not allow precise morphometrical measurements of reductions in size and dimension. Stereology, in contrast, which is an unbiased and precise method for three-dimensional measurement that has been recommended for the study of testicular structures in terms of function and reproductive capacity, can overcome the shortcomings of these techniques [17].

In addition, in most cases, cryptorchidism occurs after the testes have naturally descended (acquired cryptorchidism); in this study, however, cryptorchidism was induced surgically in infant rats. We hope that this study can provide further insights into this issue and encourage the further development of treatment strategies.

Methods

1. Experimental animals

Adult male and female Wistar rats were purchased from the Pasteur Institute, kept in an adequate environment with a 12-hour light-dark cycle and temperature range of 20 to 26 °C, and provided with *ad libitum* access to food and water. The experiment was conducted in accordance with the standard guidelines for the care and use of laboratory animals (Faculty of Veterinary Medicine, University of Tehran; no. 6860778). After the rats had adjusted to the environment, one male and two female rats were housed per cage for mating. Vaginal plaques were examined 12 hours after mating, and the pregnant rats were separated after parturition. The male offspring were then separated for this study and divided into two groups (sham and experimental).

2. Induction of cryptorchidism

Surgery was performed on the 18th postnatal day before the natural descent of the testes (rat testes descend 21 to 28 days after birth) [18,19]. Anesthesia was induced via an intraperitoneal injection of 0.1% ketamine (80 mg/kg) and 0.1% xylazine (10 mg/kg). In the experimental group, a small transabdominal incision was made on the left side. The gubernaculum was detached, and the left testis was pushed into the abdomen. The inguinal canal was then sutured to prevent the descent of the testis in order to unilaterally induce left

cryptorchidism, while the right testis was allowed to descend naturally into the scrotum. In the sham group, the abdomen was incised, and the left testis was pushed into the abdomen and released. The gubernaculum was not detached, and the inguinal canal was not closed.

The testes of five rats in each group were removed at designated time points (40, 63, and 90 days after birth) [19]. The rats were euthanized by cervical dislocation at each of the three time points, the testes were excised, and sperm analysis and stereology were undertaken to determine various parameters.

3. Sperm collection and analysis

Immediately after euthanasia, the testes were excised for stereological analysis (at three time points: 40, 63, and 90 days after birth), and the epididymis (in mature rats only, at 63 and 90 days after birth) was cut into segments, placed in phosphate-buffered saline, and incubated at 37 °C until the sperm was released from the tissue, indicating its readiness for sperm analysis.

4. Sperm count

In order to count the sperm, a 1:20 sperm solution was prepared, and 10 μL of the dilution was pipetted onto a Neubauer slide with a glass cover. The slide was placed under a light microscope with 100× magnification. The spermatozoa were then counted and recorded in millions [20].

5. Sperm morphology

To evaluate the sperm morphology, 20 μL of the supernatant containing the sperm was smeared. After the smear had dried, it was immersed in acetone-ethanol (1:1) and subsequently placed in aniline blue stain for 7 minutes. It was then observed under a light microscope at ×100 magnification, and 200 sperm cells were studied per testis [20]. Any abnormalities in either the heads or tails of the sperm were noted and classified as abnormal, and the results were presented in terms of the percentage of normal and abnormal spermatozoa using a similar procedure to that described previously [21].

6. Sperm tail length

Systematic uniform random fields of view were chosen by maintaining equal distances on the X and Y axes, and 200 sperm cells were studied per testis. A Merz grid with defined measurements was superimposed onto the computer monitor, and a calculation was made using the following formula [22]:

$$\sum L = (\pi/2) \times (a/l) \times (1/asf) \times \sum I$$
$$L = \sum L / \sum N$$

where "a/l" is the Merz grid constant, which was acquired as follows. The area of each basic tile (smaller frame) was calculated by multiplying the length and width of said tile (xy). Within this tile, there were two semicircles with lengths of pd (circumference of the circle), where "d" was the diameter of 1 semicircle. Therefore, the Merz grid constant "a/l" was calculated as (XY)/pd. "asf" refers to the area of the basic tile divided by the area of the counting frame (larger frame). "$\sum I$" was the total number of intersections between the sperm tails and the semicircles. "$\sum N$" was the total number of the counted sperm cells in the unbiased counting frame.

In order for sperm to be counted, the sperm head had to be located inside the counting frame or on the inclusion lines (green lines) (Figure 1).

7. Tissue sampling and stereological methods

On the designated date for each group and following euthanasia, both testes were removed, weighed, and immersed in a 10% formalin solution for fixation. Following this procedure, each testis was embedded in an agar block to obtain isotropic uniform random slabs. The agar block containing the testis was randomly placed at the center of a circle with 90 equidistant divisions along its perimeter, a random number between 0 and 90 was generated and the block was cut along a line parallel to the direction of the selected number. The block was placed on its cut surface at the center of a second equiangular circle, with 96 non-equidistant divisions along its perimeter. The agar block was then divided into different slabs by using a tissue slicer to cut it along a line that was parallel to the direction of a ran-
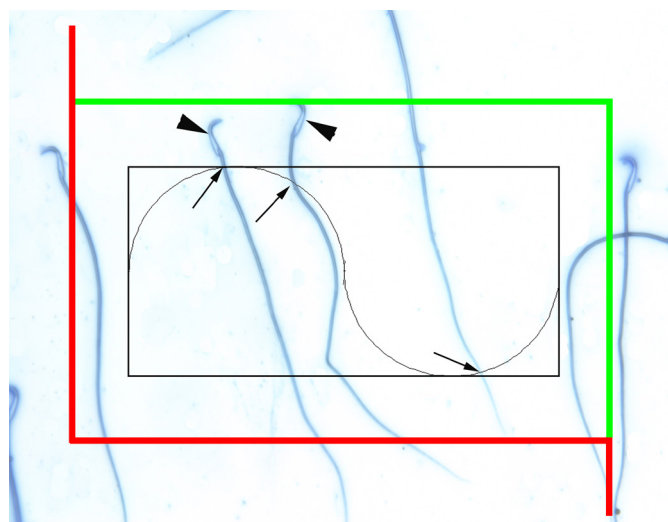
Figure 1. Calculation of sperm tail length using a Merz grid. The arrowheads indicate counted sperms, whereas the arrows indicate the intersections between the sperm tails and the semicircles (aniline blue staining, ×400 magnification).

dom number ranging from 0 to 96 (Figure 2). These slabs were ultimately embedded in paraffin while placed on their cut surfaces after routine histological processing. Sections with a thickness of 5 μm were then cut with a microtome and stained with hematoxylin and eosin. The slides were observed using an Olympus light microscope (CX40, Olympus) connected to a digital camera (MB-225). Systematic uniform random fields of view were captured by moving the microscope stage in equal distances in the x and y directions for each section.

8. Volume estimation

The total volume of the testis was calculated based on its weight. The images were analyzed using a dedicated software program (ImageJ; https://imagej.nih.gov) and specific plugins. In order to calculate the testicular volume fractions of seminiferous tubules and interstitial tissue and the epithelial volume, a test point system was implemented by applying the below formula (Figure 3A) [23]:

$$V_v \text{ (structure)} = \sum P \text{ (structure)} / \sum P \text{ (testis)}$$

where "V_v" is the volume fraction of testicular structures, "$\sum P$ (structure)" is the total number of test points overlying the specific testicular structure, and "$\sum P$ (testis)" is the total number of points overlying the entire testis. The total volume of each structure was calculated by multiplying the volume fraction by the total volume of the testis.

9. Surface area estimation

The surface density of the germinal layer was calculated using test line probes and the following formula (Figure 3B) [24]:

$$S_v = \frac{2 \times \sum I}{l/p \times \sum P}$$

where "$\sum I$" is the number of intersections between the test lines and the luminal surface of the germinal layer, "l/p" is the length of each test line associated with each point of the test grid, and "$\sum P$" is the number of points overlying the germinal layer. The total surface area of the germinal layer was ultimately calculated by multiplying the surface density by the volume of the germinal epithelium.
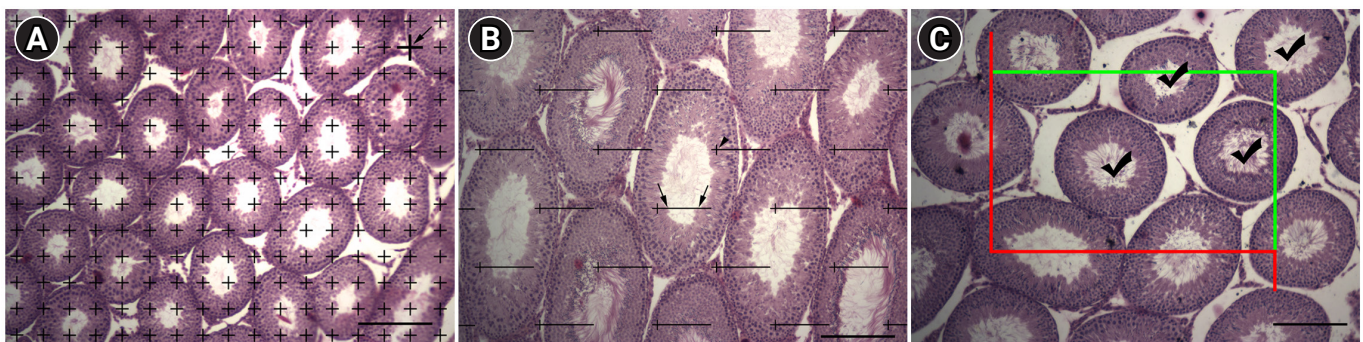
10. Length of seminiferous tubules

The length of the seminiferous tubules was estimated by superimposing an unbiased counting frame onto each microscopic field of view. The tubule profiles located inside the counting frame or crossing the inclusion lines (green lines) were counted (Figure 3C), and the length density was calculated as follows:

$$L_v \text{ (seminiferous tubules)} = 2\sum Q / (\sum P \times a/p)$$

J Sadeghinezhad et al.   Rat cryptorchid testis stereology

CERM
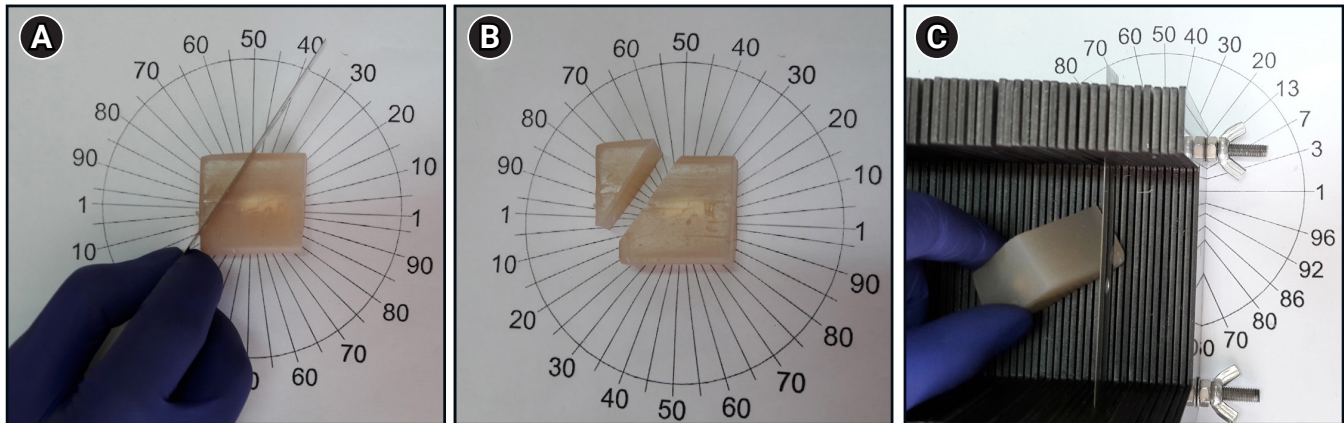
Figure 2. Isotropic, uniform random sections of the rat testes were obtained by applying the orientator method. (A) The testis for each animal was embedded in an agar block and placed at the center of a circle with 90 equidistant divisions along the perimeter. A random number between 0 and 90 was chosen. (B) The agar medium was cut along a parallel line according to the direction of the selected number (here, 35). (C) The agar block was placed on its cut surface at the center of a second circle, with 96 non-equidistant divisions along its perimeter. The agar was cut into multiple equidistant pieces along a parallel line according to the direction of a random number from 0 to 96 (here, 50) using a tissue slicer.

Figure 3. Estimation of testicular volume, testicular surface area, and the length of the seminiferous tubules. (A) Estimation of testicular volume by employing the point-counting system. The volume of testicular structures was estimated by randomly superimposing a point-counting probe onto each section. The upper-right corner of each point (arrow) was used as a reference to count the number of points hitting the targeted region of interest (hematoxylin-eosin stain, scale bar: 200 µm). (B) Calculation of the surface area of seminiferous tubules using test line probes randomly superimposed onto each section. The test points hitting the seminiferous tubule epithelium (arrowhead) and the points where test lines and the seminiferous tubule lumen intersect (arrows) were counted (hematoxylin-eosin staining, scale bar: 200 µm). (C) The unbiased counting frame principle was applied to estimate the length of the seminiferous tubules. The profiles located inside the counting frame or crossing the inclusion lines (green lines) were counted (hematoxylin-eosin staining, scale bar: 200 µm).

where "ΣQ" is the total number of the counted profiles, "ΣP" is the total number of counted frames, and "a/p" is the area per frame [23]. The total length was subsequently obtained by multiplying the length density by the total volume of the testis.

11. Statistical analysis

SPSS version 27 (IBM Corp.) was used to conduct the statistical analysis, and the normality of the distribution of the data was analyzed using the Kolmogorov-Smirnov test. The Kruskal-Wallis and Mann-Whitney tests were used for statistical analysis of the sperm count. One-way analysis of variance and the Tukey test were used to analyze the sperm morphology, sperm tail length, and stereological parameters. A p-value of <0.05 was considered to indicate statistical significance.

Results

1. Sperm count

Observations of the left testes at 63 and 90 days revealed that the sham group had a higher sperm count than the experimental group

(p<0.05), whereas hardly any differences in the right testes were observed between the groups (p>0.05) (Figure 4).
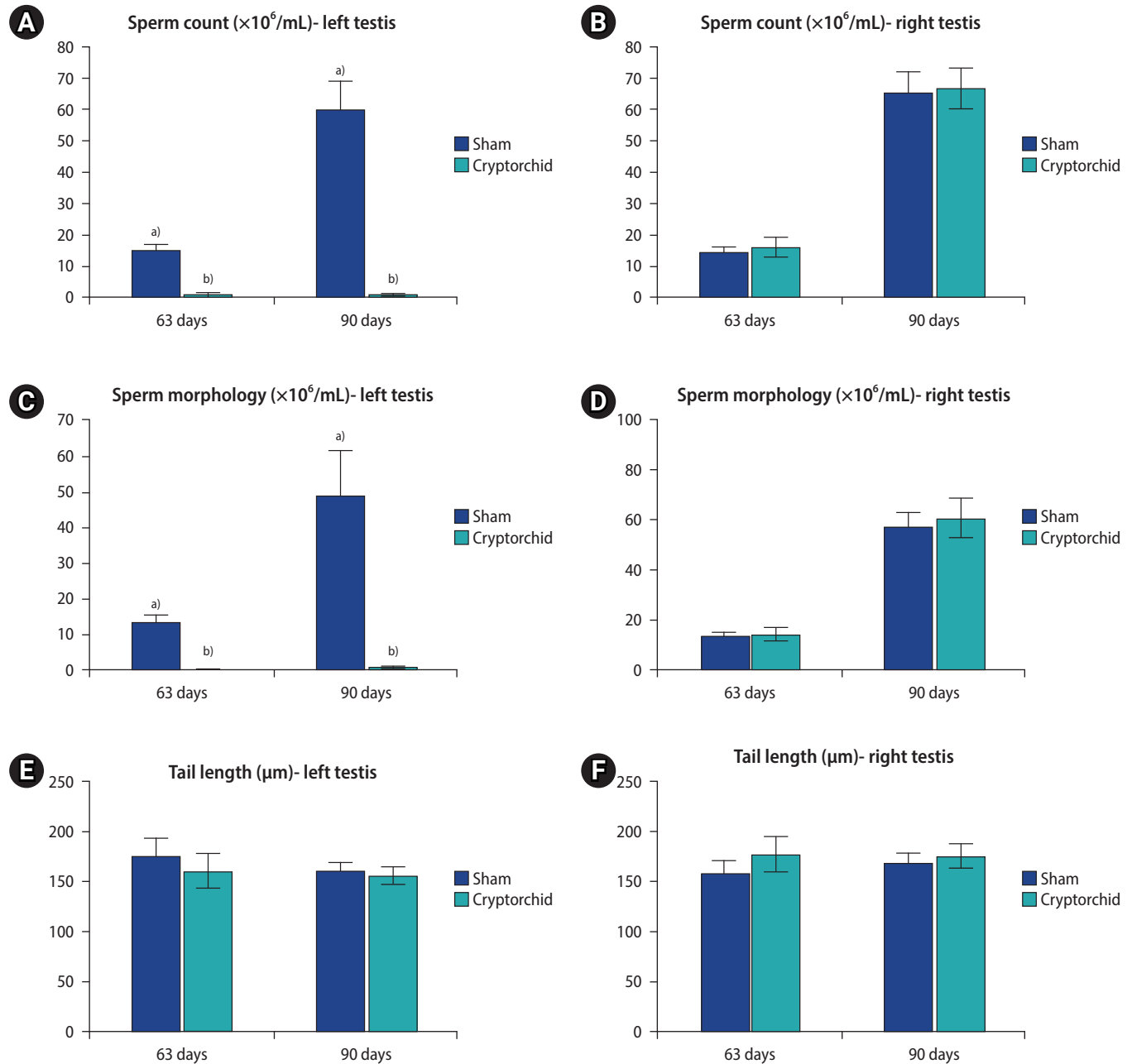
2. Sperm morphology

In the testes at 63 and 90 days, the normal sperm count was considerably higher in the sham group than in the experimental group (p<0.05). However, no major differences in the right testes were observed between the sham and experimental groups (p>0.05) (Figure 4).

3. Sperm tail length

The sperm tail length in the left testes did not vary between the sham and experimental groups at both 63 and 90 days (p>0.05). The same results were observed for the right testes (Figure 4).

4. Total testicular volume and fractional volumes of seminiferous tubules, interstitial tissue, and epithelium

The calculated volumes of the various parameters are summarized

Figure 4. Comparison of (A, B) sperm count, (C, D) normal sperm morphology, and (E, F) sperm tail length at 63 and 90 days in the sham and experimental (cryptorchid) groups. [a),b)]Significant differences between the groups are indicated with different letters (p<0.05).

J Sadeghinezhad et al.   Rat cryptorchid testis stereology

CERM ■

in Table 1. Total testicular volume and the fraction of volume of the seminiferous tubule were significantly lower in the left testes of the experimental group than in the right and left testes of the sham group and the right testes of the experimental group at all time points ($p<0.05$). The fraction of volume of interstitial tissue was also greater in the left testes of the experimental group than in the other groups at all ages ($p<0.05$). Furthermore, the epithelial volume fraction of the left testes at 40 days in the experimental group was significantly lower than that of the testes in the other groups ($p<0.05$).

5. Epithelial surface area and tubular length

The values for epithelial surface area and seminiferous tubule length are reported in Table 2. Based on the results, the total epithelial surface area and seminiferous tubule length were found to be significantly lower in the left testes of the experimental group than in the right and left testes of the sham group and the right testes in the experimental group at all time points ($p<0.05$).

Discussion

This is the first study to report three-dimensional quantitative data regarding testicular morphometry using unbiased design-based stereology in rat testes following experimentally-induced cryptorchidism. Cryptorchidism can damage the germinal epithelium, decrease the concentration of healthy sperm, reduce semen quality, and eventually lead to sperm disorders such as immaturity, necrosis, and apoptosis [25]. The heat stress that cryptorchid testes undergo increases the ROS, which in turn induces apoptosis of spermatogenic cells and decreases sperm motility by attacking the sperm DNA [8].

As expected, the sperm count and the number of sperms with normal morphology were significantly lower in the left testes with induced cryptorchid in the experimental group than in the testes of the other groups at all ages. Greater mid-piece sperm length indicating increased levels of mitochondria, along with greater sperm tail length, is associated with increased sperm motility (and viability) and normal sperm morphology, which ultimately influence fertility [22,26]. Increased mid-piece sperm tail length corresponding to the

Table 1. Total testicular volume and volume fractions of testicular structures in rat testes at 40, 63, and 90 days

Parameter	Age (day)	Sham group		Experimental group	
		Right	Left	Right (scrotal)	Left (abdominal)
Total testicular volume (cm³)	40	0.58±0.07[a]	0.60±0.04[a]	0.53±0.04[a]	0.29±0.02[b]
	63	1.39±0.09[a]	1.41±0.08[a]	1.32±0.15[a]	0.41±0.07[b]
	90	1.28±0.17[a]	1.23±0.12[a]	1.39±0.16[a]	0.45±0.07[b]
Interstitial volume (%)	40	25.98±2.19[a]	24.08±3.75[a]	25.35±2.98[a]	36.18±3.32[b]
	63	26.48±1.05[a]	27.04±1.29[a]	25.22±1.67[a]	33.18±1.68[b]
	90	25.29±3.55[a]	27.06±3.13[a]	27.58±2.24[a]	38.70±6.53[b]
Epithelium volume (%)	40	56.78±2.51[a]	58.46±3.54[a]	55.08±2.19[a]	42.43±2.95[b]
	63	53.15±2.66[a]	53.98±2.14[a]	53.55±1.44[a]	50.62±4.77[a]
	90	54.69±2.80[a]	55.50±4.03[a]	54.17±4.27[a]	52.41±4.86[a]
Seminiferous tubule volume (%)	40	74±2.19[a]	75.89±3.74[a]	74.63±2.98[a]	63.80±3.32[b]
	63	74.51±2.19[a]	72.95±1.29[a]	75.92±2.01[a]	66.81±1.68[b]
	90	74.69±3.55[a]	72.92±3.13[a]	72.40±2.24[a]	61.28±6.53[b]

Values are presented as mean±standard deviation.
[a),b)]Different letters in each row indicate significant differences between the groups ($p<0.05$).

Table 2. Epithelial surface area and tubular length in rat testes at 40, 63, and 90 days

Parameter	Age (day)	Sham group		Experimental group	
		Right	Left	Right (scrotal)	Left (abdominal)
Epithelial surface area (cm²)	40	27.08±3.76[a]	30.40±6.41[a]	23.71±4.50[a]	11.13±2.58[b]
	63	62.68±5.74[a]	60.25±2.01[a]	65.00±11.81[a]	21.83±8.71[b]
	90	59.98±12.87[a]	61.26±16.34[a]	68.47±3.03[a]	27.04±13.19[b]
Seminiferous tubule length (m)	40	13.58±0.73[a]	15.56±0.87[a]	13.54±1.25[a]	10.65±2.03[b]
	63	20.91±5.29[a]	22.27±2.00[a]	24.34±3.90[a]	12.87±3.07[b]
	90	19.67±2.63[a]	22.15±3.62[a]	23.40±2.00[a]	13.13±1.39[b]

Values are presented as mean±standard deviation.
[a),b)]Different letters in each row indicate significant differences between the groups ($p<0.05$).

mitochondrial sheath, which is responsible for energy production and velocity, has a known association with a significant increase in the mean conception rate and better sperm parameters, such as a higher percentage of viable and intact acrosomes [27]. However, compared to previous studies, in the present study, the sperm tail length in the cryptorchid testes was, although lower, not significantly different from that of the eutopic testes in the sham group.

Previous studies have shown that evaluating testicular volume is one of the most efficient indirect ways to predict fertility in men, especially in pediatric patients where semen analysis is not feasible [28]. Evaluation of the total testicular volume positively predicts male fertility due to its association with seminiferous tubule content, particularly the testosterone-secreting compartment, especially when performed alongside an ultrasonographic assessment of testicular parenchymal homogeneity, indicating normal semen quality and normozoospermia [29]. Cryptorchidism results in the incomplete formation of seminiferous tubules and interstitial tissue [30] and causes a massive depletion of spermatogenic cells [1]. Since 80% to 90% of the testis consists of seminiferous tubules, testicular volume depends on the process of spermatogenesis [31]. In addition, the testicular volume of cryptorchid testes considerably decreases after 6 months of age, and a correlation has been observed between testicular volume and the duration of the anomaly as well as the location of the cryptorchid testis in terms of its distance from the scrotum [31]. In this study, the total testicular volume and volume of the seminiferous tubules were significantly lower in the cryptorchid testes at all ages compared to the testes in the sham group. A stereological study on experimentally-induced cryptorchidism in rabbits reported similar results and observed a significant decrease in the volume of the seminiferous tubules and, consequently, in the total testicular volume in the cryptorchid testes [32].

Intra-abdominal testes are predisposed to seminiferous tubule alterations. These alterations depend on the thickness of the lamina propria, which may interfere with metabolic exchanges between the seminiferous tubules and the interstitial tissue [33], and on the level of degenerative changes in the immature Sertoli cells [30]. Moreover, cryptorchid testes are subject to elevated temperatures, which causes heat stress leading to oxidative damage [8], excessive germ cell death [34], and altered seminiferous epithelial cycles [1]. In addition, following oxidative stress, the decrease in the surface area of the seminiferous epithelium can be attributed to the extension of the G1 phase in spermatogonium B mitosis, which eventually restrains the growth cycle of the cell [35]. Decreased intratesticular testosterone (due to a decrease in the number of Leydig cells) may trigger the production of multinucleated giant cells [36], which are linked to cell apoptosis and represent a marker for the cryptorchid seminiferous epithelium [1]. The fraction of the volume of the seminiferous tu-

bules was reduced in the left cryptorchid testis in the experimental group at all ages. However, the seminiferous tubule epithelial volume decreased at 40 days only. Given that the proliferation of spermatogenic cells increases before and during puberty [37], the decrease in the epithelial volume observed at this age can therefore be explained.

Cryptorchidism leads to increased interstitial tissue volume and increased fibrosis in the testes [38]. This phenomenon has been explained by the increased number of mast cells, which are known to play a role in fibrosis in the interstitial and subtubular areas of unilaterally undescended testes in cryptorchid and infertile testes [39]. In this study, greater interstitial volumes were consistently observed in the cryptorchid testes compared to the other groups. Our findings are consistent with a previous study on cryptorchid calves in which the hypoplastic cryptorchid testes presented an increased number of interstitial endocrine cells, marked fibrosis, and arrested spermatogenesis [40].

After birth, the seminiferous tubules start to gradually increase in length, become more compact, and ultimately form a dense structure. The length of seminiferous tubules and their structure influences spermatogenic cell growth and the movement of sperm towards the epididymis [41]. Accordingly, reduced total testicular volume that is secondary to cryptorchidism can influence tubular length [41] and eventually alter normal functions and induce infertility. A stereological study carried out on rabbit testes following experimentally-induced unilateral cryptorchidism reported a significant decrease in both total testicular volume and tubular length and diameter [32], which was similar to the findings of this study. In the present study, along with reduced total testicular volume, the length of the seminiferous tubules was lower in the abdominal cryptorchid testes only.

Histologically, the seminiferous tubules of cryptorchid testes tend to show structural abnormalities, such as increased tubule branching and tubular blind ends, smaller tubular diameter, and areas completely free of germ cells, as opposed to normally descended testes, which have evenly distributed spermatogonia and regular tubular morphology. The structural abnormalities seen in cryptorchid testes suggest that injury tends to occur early in testicular development [42]. Both the diameter and length of seminiferous tubules are indicators of morphological testicular value, and both parameters have been reported to be significantly lower in ectopic testicles than in orthotopic testicles at any given age [43,44], as seen in the present study for the length and epithelial surface area of seminiferous tubules.

Studies have observed damage in the contralateral testis as a result of unilateral cryptorchidism, especially spermatogonia cell depletion, which, once present, is irreversible even after orchiopexy

J Sadeghinezhad et al.   Rat cryptorchid testis stereology

CERM

[45,46]. A decreased spermatogonia per tubule ratio has been reported in both the unilateral cryptorchid testis and the corresponding contralateral descended testis, with the extent of the change in the ectopic testis strictly corresponding to that of the contralateral testis. The impaired transition from gonocytes into Ad-type spermatogonia is the etiopathological origin of the defect, which explains the azoospermia and infertility disorders seen in adult men with unilateral cryptorchidism [15]. In the present study, no significant differences were observed between the parameters measured in the scrotal contralateral testes in the experimental groups and the normal eutopic testes in the sham group. In other words, the contralateral scrotal testes in the experimental group were seemingly unaffected in terms of their structural morphology by the unilateral cryptorchidism condition experimentally-induced in this study. This may have been a result of the surgical inducement of cryptorchidism in this study [47]. A study on rabbits that had undergone experimentally-induced unilateral cryptorchidism showed similar findings in the contralateral testis to the cryptorchid testis. Spermatocyte counts; the volume, diameter, and length of seminiferous tubules; and the total testicular volume were not significantly different in the experimental testes compared to the control testes [32]. In addition, a notable study on bucks with natural unilateral cryptorchidism further confirmed how the lengths, heights, and diameters of the seminiferous tubules in the contralateral testes are significantly higher than the retained testes, and that the percentage of spermatogenic cells per testis did not differ from those calculated in normal control bucks. Additionally, higher volumes of Leydig cells and seminiferous tubules in the contralateral scrotal testes were observed compared to the bucks with normal testes, indicating that the spermatogenic efficiency of the scrotal testes of bucks with unilaterally cryptorchid testes was higher than that of the control bucks [48]. These data further support our hypothesis that the contralateral scrotal testis in cases of unilateral cryptorchidism retains its reproductive potential.

In conclusion, although the effects of cryptorchidism are well known, this abnormality is still a major challenge that affects male fertility. In order to devise optimal treatment measures, this condition must be better understood. This study aimed to provide a better understanding of cryptorchidism by precisely measuring the biological features of cryptorchid testes as a whole. The results confirmed that the total volume of the testis and the volume of the seminiferous tubules decrease due to cryptorchidism, while the volume of the interstitial tissue increases. In addition, the length of the seminiferous tubules and the surface area of the germinal epithelium of the seminiferous tubules decrease due to cryptorchidism. These changes were observed at all examined time points but did not affect the opposite testis.

Conflict of interest

No potential conflict of interest relevant to this article was reported.

ORCID

Javad Sadeghinezhad	https://orcid.org/0000-0003-0735-8788
Fatemeh Yarmahmoudi	https://orcid.org/0000-0001-7206-8969
Mohammad Mehdi Dehghan	https://orcid.org/0000-0002-8825-9070
Saeed Farzad Mohajeri	https://orcid.org/0000-0003-4694-347X
Ehsan Roomiani	https://orcid.org/0000-0002-4877-9119
Hadis Bojarzadeh	https://orcid.org/0000-0001-9036-6871
Mahdi Aghabalazadeh Asl	https://orcid.org/0000-0002-0679-808X
Ava Saeidi	https://orcid.org/0009-0006-0684-6797
Margherita De Silva	https://orcid.org/0000-0003-0627-4427

Author contributions

Conceptualization: JS, MMD. Data curation: ER, MAA, AS. Formal analysis: JS. Methodology: JS, MMD, SFM. Writing-original draft: JS, FY, HB. Writing-review & editing: JS, MDS.

References

1. Zheng Y, Zhang P, Zhang C, Zeng W. Surgery-induced cryptorchidism induces apoptosis and autophagy of spermatogenic cells in mice. Zygote 2019;27:101-10.
2. Elder JS. Surgical management of the undescended testis: recent advances and controversies. Eur J Pediatr Surg 2016;26:418-26.
3. Aitken RJ, Baker MA. Causes and consequences of apoptosis in spermatozoa: contributions to infertility and impacts on development. Int J Dev Biol 2013;57:265-72.
4. Barthold JS, Gonzalez R. The epidemiology of congenital cryptorchidism, testicular ascent and orchiopexy. J Urol 2003;170(6 Pt 1):2396-401.
5. Trsinar B, Muravec UR. Fertility potential after unilateral and bilateral orchidopexy for cryptorchidism. World J Urol 2009;27:513-9.
6. Gurney JK, McGlynn KA, Stanley J, Merriman T, Signal V, Shaw C, et al. Risk factors for cryptorchidism. Nat Rev Urol 2017;14:534-48.
7. Aitken RJ, Curry BJ. Redox regulation of human sperm function: from the physiological control of sperm capacitation to the etiology of infertility and DNA damage in the germ line. Antioxid Redox Signal 2011;14:367-81.
8. Avci V, Ayengin K, Alp HH. Oxidative DNA damage and NOX4 levels in children with undescended testes. Eur J Pediatr Surg 2019; 29:545-50.

9. Makker K, Agarwal A, Sharma R. Oxidative stress & male infertility. Indian J Med Res 2009;129:357-67.

10. Cocco C, Brancia C, Corda G, Ferri GL. The hypothalamic-pituitary axis and autoantibody related disorders. Int J Mol Sci 2017;18: 2322.

11. Trabert B, Zugna D, Richiardi L, McGlynn KA, Akre O. Congenital malformations and testicular germ cell tumors. Int J Cancer 2013; 133:1900-4.

12. Urh K, Kunej T. Molecular mechanisms of cryptorchidism development: update of the database, disease comorbidity, and initiative for standardization of reporting in scientific literature. Andrology 2016;4:894-902.

13. Vinardi S, Magro P, Manenti M, Lala R, Costantino S, Cortese MG, et al. Testicular function in men treated in childhood for undescended testes. J Pediatr Surg 2001;36:385-8.

14. Cortes D. Cryptorchidism: aspects of pathogenesis, histology and treatment. Scand J Urol Nephrol Suppl 1998;196:1-54.

15. Verkauskas G, Malcius D, Dasevicius D, Hadziselimovic F. Histopathology of unilateral cryptorchidism. Pediatr Dev Pathol 2019;22: 53-8.

16. Ge WL, Chen JN, Ji LH, Zhao J, Xian H, Xu YZ. NEK2 gene expression in mouse cryptorchidism model and its mechanism involved in apoptosis. Zhonghua Yi Xue Za Zhi 2020;100:3534-8.

17. Sadeghinezhad J, Ganji Z, Sadeghian Chaleshtori S, Bojarzadeh H, Aghabalazadeh Asl M, Khomejini AB, et al. Morphometric study of the testis in sheep embryos using unbiased design-based stereology. Anat Histol Embryol 2021;50:1026-33.

18. Kocak I, Dundar M, Hekimgil M, Okyay P. Assessment of germ cell apoptosis in cryptorchid rats. Asian J Androl 2002;4:183-6.

19. Mirilas P, Psalla D, Mentessidou A. A diagnostic model for histologic damage in undescended testes based on testis rigidity measurement: an experimental study with a novel device. J Surg Res 2014;192:521-30.

20. World Health Organization. WHO laboratory manual for the examination and processing of human semen. 5th ed. WHO; 2010.

21. Narayana K, D'Souza UJ, Seetharama Rao KP. Ribavirin-induced sperm shape abnormalities in Wistar rat. Mutat Res 2002;513: 193-6.

22. Noorafshan A, Karbalay-Doust S. A simple method for unbiased estimating of ejaculated sperm tail length in subjects with normal and abnormal sperm motility. Micron 2010;41:96-9.

23. Gundersen HJ, Bendtsen TF, Korbo L, Marcussen N, Moller A, Nielsen K, et al. Some new, simple and efficient stereological methods and their use in pathological research and diagnosis. APMIS 1988;96:379-94.

24. Howard V, Reed M. Unbiased stereology: three-dimensional measurement in microscopy. Garland Science; 2004.

25. Moretti E, Di Cairano G, Capitani S, Scapigliati G, Baccetti B, Collodel G. Cryptorchidism and semen quality: a TEM and molecular study. J Androl 2007;28:194-9.

26. Gu NH, Zhao WL, Wang GS, Sun F. Comparative analysis of mammalian sperm ultrastructure reveals relationships between sperm morphology, mitochondrial functions and motility. Reprod Biol Endocrinol 2019;17:66.

27. Kerns K, Jankovitz J, Robinson J, Minton A, Kuster C, Sutovsky P. Relationship between the length of sperm tail mitochondrial sheath and fertility traits in boars used for artificial insemination. Antioxidants (Basel) 2020;9:1033.

28. Varela-Cives R, Mendez-Gallart R, Estevez-Martinez E, Rodriguez-Barca P, Bautista-Casasnovas A, Pombo-Arias M, et al. A cross-sectional study of cryptorchidism in children: testicular volume and hormonal function at 18 years of age. Int Braz J Urol 2015;41:57-66.

29. Spaggiari G, M Granata AR, Santi D. Testicular ultrasound inhomogeneity is an informative parameter for fertility evaluation. Asian J Androl 2020;22:302-8.

30. Pinart E, Sancho S, Briz M, Bonet S. Morphologic study of the testes from spontaneous unilateral and bilateral abdominal cryptorchid boars. J Morphol 1999;239:225-43.

31. Zvizdic Z, Milisic E, Halimic A, Zvizdic D, Zubovic SV. Testicular volume and testicular atrophy index as predictors of functionality of unilaterally cryptorchid testis. Med Arch 2014;68:79-82.

32. Zhang RD, Wen XH, Kong LS, Deng XZ, Peng B, Huang AP, et al. A quantitative (stereological) study of the effects of experimental unilateral cryptorchidism and subsequent orchiopexy on spermatogenesis in adult rabbit testis. Reproduction 2002;124:95-105.

33. Hadziselimovic F, Girard J. Pathogenesis of cryptorchidism. Horm Res 1977;8:76-83.

34. Zhu H, Cui Y, Xie J, Chen L, Chen X, Guo X, et al. Proteomic analysis of testis biopsies in men treated with transient scrotal hyperthermia reveals the potential targets for contraceptive development. Proteomics 2010;10:3480-93.

35. Jedlinska-Krakowska M, Bomba G, Jakubowski K, Rotkiewicz T, Jana B, Penkowski A. Impact of oxidative stress and supplementation with vitamins E and C on testes morphology in rats. J Reprod Dev 2006;52:203-9.

36. Barqawi A, Trummer H, Meacham R. Effect of prolonged cryptorchidism on germ cell apoptosis and testicular sperm count. Asian J Androl 2004;6:47-51.

37. Pereira MR, Aleixo JF, Cavalcanti LF, Costa NO, Vieira ML, Ceravolo GS, et al. Can maternal exposure to paracetamol impair reproductive parameters of male rat offspring? Reprod Toxicol 2020; 93:68-74.

J Sadeghinezhad et al.   Rat cryptorchid testis stereology

CERM

38. Shin HJ, Lee YS, Yoon H, Kim MJ, Han SW, Kim HY, et al. Testicular volume and elasticity changes in young children with undescended testes. Med Ultrason 2017;19:380-5.

39. Acikgoz A, Asci R, Aydin O, Cavus H, Donmez G, Buyukalpelli R. The role of ketotifen in the prevention of testicular damage in rats with experimental unilateral undescended testes. Drug Des Devel Ther 2014;8:2089-97.

40. Fuke N, Kitahara G, Ito S, Van Diep N, Ping Teh AP, Izzati UZ, et al. Severe degenerative changes in cryptorchid testes in Japanese black cattle. Vet Pathol 2020;57:418-26.

41. Jezek D, Simunic-Banek L, Pezerovic-Panijan R. Effects of high doses of testosterone propionate and testosterone enanthate on rat seminiferous tubules: a stereological and cytological study. Arch Toxicol 1993;67:131-40.

42. Knecht H. Tubular structure and germ cell distribution of cryptorchid or normal testes in early childhood (author's transl). Beitr Pathol 1976;159:249-70.

43. Kleinteich B, Schickedanz H. Length-growth of seminiferous tubules of untreated and as surgically displaced, congenitallydystopic testes in children and adolescents. Z Urol Nephrol 1977;70:501-9.

44. Kleinteich B, Schickedanz H. Studies on the growth of the width in seminiferous tubules of eutopic and congenitally dystopic testes in children and adolescents. Z Urol Nephrol 1977;70:491-500.

45. Patkowski D, Czernik J, Jelen M. The natural course of cryptorchidism in rats and the efficacy of orchidopexy or orchidectomy in its treatment before and after puberty. J Pediatr Surg 1992;27:870-3.

46. Zivkovic D, Bica DG, Hadziselimovic F. Effects of hormonal treatment on the contralateral descended testis in unilateral cryptorchidism. J Pediatr Urol 2006;2:468-72.

47. Zakaria O, Shono T, Imajima T, Suita S. Comparative studies of fertility and histologic development of contralateral scrotal testes in two rat models of unilateral cryptorchidism. Pediatr Surg Int 2000;16:498-501.

48. Okpe GC, Ezeasor DN. Influence of naturally unilateral cryptorchidism on the histomorphometry of the testes and daily sperm production in West African Dwarf goats. Iran J Vet Res 2016;17:13-9.